Mechanism of Reaction in NaAlCl4 Molten Salt Batteries with Nickel Felt Cathodes and Aluminum Anodes. Part II: Experimental Results and Comparison with Model Calculations.

Knutz, B.C.; Berg, Rolf W.; Hjuler, Hans Aage; Bjerrum, Niels

Published in:
Journal of The Electrochemical Society

Link to article, DOI:
10.1149/1.2221099

Publication date:
1993

Document Version
Publisher's PDF, also known as Version of record

Mechanism of Reaction in $NaAlCl_4$ Molten Salt Batteries with Nickel Felt Cathodes and Aluminum Anodes

II. Experimental Results and Comparison with Model Calculations

B. C. Knutz,[a] R. W. Berg, H. A. Hjuler,* and N. J. Bjerrum*

Molten Salts Group, Chemistry Department A, The Technical University of Denmark, DK-2800 Lyngby, Denmark

ABSTRACT

The battery systems: Al/NaCl-$AlCl_3$-Al_2X_3/Ni-felt (X = S, Se, Te) and the corresponding system without chalcogen have been studied experimentally at 175°C. Charge/discharge experiments, performed on cells with NaCl saturated melts, show that advantages with regard to rate capability and cyclability can be obtained with systems containing dissolved chalcogen compared with the chalcogen-free system. Exchange of chalcogen between cathode and electrolyte during cycling was confirmed by performing gravimetric analysis and Raman spectroscopy of the electrolytes. Cathode reactions were studied by coulometric titrations (performed on cells with slightly acidic NaCl-$AlCl_3$ melts and small amounts of chalcogen) and compared with model calculations. Cells containing chalcogen revealed at least three voltage plateaus during cycling. The lowest plateau is associated with formation/decomposition of essentially Ni_yS_z and Ni_ySe_z in the sulfide and selenide system, respectively. Cells containing selenide revealed extra capacity below the Ni_ySe_z-plateau, most probably associated with a $Al_vNi_ySe_z$ compound. On the second plateau of sulfide systems $NiCl_2$ or a $Ni_yS_zCl_{2y-2z}$ compound with $y > (4.4 \pm 0.2) \cdot z$ is formed during charging. Reduction of the formed compound to Ni takes place via consumption of sodium chloride. For acidic melts, sulfide at the cathode was found to be present as 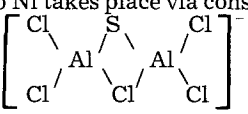 species.

It is well-known that there is a marked need for improved rechargeable batteries, *e.g.*, for load-leveling and traction purposes. The battery Al/NaCl-$AlCl_3$-Al_2S_3/Ni-felt (175°C) or the corresponding system with a liquid sodium-anode and a Na^+ conducting separator may turn out as candidates for these applications.

We have in the preceding paper (Part I[1]) presented a model describing thermodynamic properties of the above mentioned battery system.

Here we report experimental results obtained with cells in which the cathode material is formed *in situ* during cycling. The cells had a pure nickel metal felt cathode in contact with a NaCl-$AlCl_3$ melt to which eventually was added elemental sulfur or a sulfur containing compound. Experiments were also performed on cells containing selenium and tellurium.

It is known[2] that sulfur, selenium, and perhaps tellurium can react with aluminum in chloroaluminate melts according to the reactions

$$2Al + 3X \rightarrow \text{“}Al_2X_3\text{”} \quad [1a]$$

or

$$2Al + 3X + 2NaCl + NaAlCl_4 \rightarrow 3\text{“}NaAlXCl_2\text{”} \quad [1b]$$

where X = S, Se, and perhaps Te. “Al_2X_3” and “$NaAlXCl_2$” are apparent formulas, since the chalcogens probably exist in the form of polymeric species in NaCl-$AlCl_3$ melts. Furthermore, elemental chalcogens may be reduced by reaction with nickel forming chalcogenides, resulting in a partly charged cell instead of a discharged cell.

Results from several sets of experiments are reported. We first carried out charge/discharge tests. In order to investigate the positive electrode reactions, gravimetric analyses, Raman studies, and potentiometric measurements were performed.

Experimental

Common experimental conditions.—The experimental cells used in this work are shown in Fig. 1 and 2. They were made of borosilicate glass. Aluminum metal (99.999% from Atomergic Chemetals Corporation) and nickel felt (from Sorapec, France[3,4]) were used for the anode and cathode, respectively, with aluminum employed in excess. The anodes were fabricated as cylinders (height 1 to 1.5 cm, diameter ~0.5 cm). Rigid tungsten wires (diameter 0.1 cm), which served as current collectors, were squeezed into a drilled hole in the cylinders. Surface impurities arising from the machining of aluminum were removed by treating the anodes in a concentrated NaOH solution. To minimize the surface oxide present, the anodes were further treated in a 12:10:3 mixture by volume of concentrated H_3PO_4, H_2SO_4, and HNO_3 acids, respectively, and finally cleaned with distilled water. Cells were washed with distilled water, dried at 150°C for about 24 h, leak-tested, and finally loaded with chemicals.

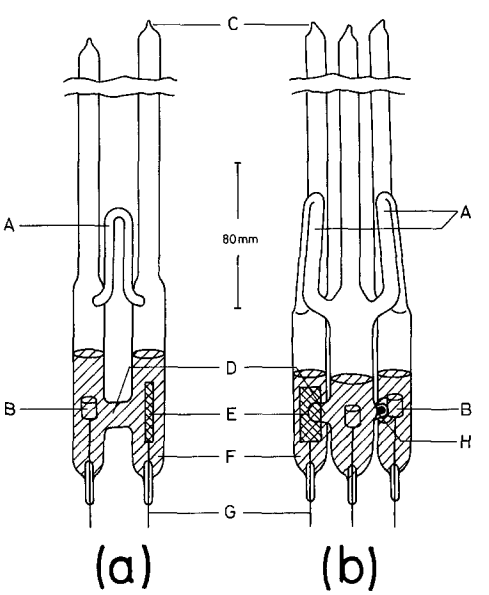

Fig. 1. (a) Battery cell, (b) three-chamber cell used for potentiometric measurements: A, pressure equilibrating tubes; B, aluminum anodes; C, sealing positions; D, main chambers of cells; E, nickel felt cathodes; F, electrolyte; G, current collectors (tungsten wires); H, porous diffusion separator.

* Electrochemical Society Active Member.

[a] Present address: Randersgade 11, 2. th., DK-2100 København ø, Denmark.

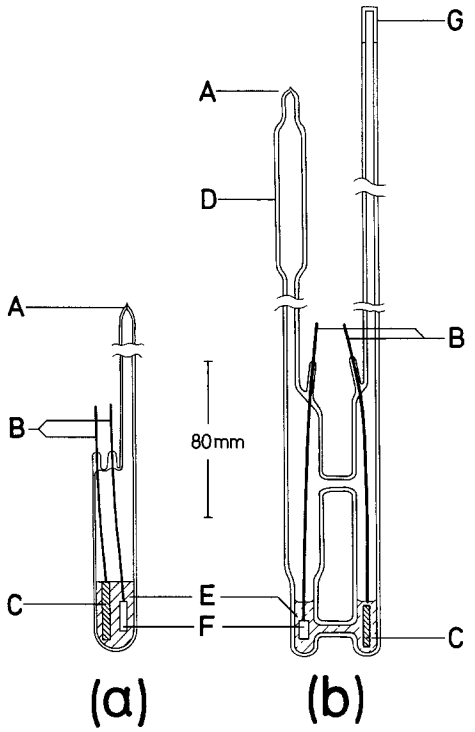

Fig. 2. Raman spectroscopy cells, (a) shaped to fit into the Raman furnace, (b) designed with a greater electrode distance to avoid dendrite formation: A, sealing positions; B, current collectors (tungsten wires); C, nickel felt cathodes; D, bulb allowing for electrolyte exchange; E, electrolyte; F, aluminum anodes; G, cuvette section, introduced in the Raman furnace when performing spectral measurements.

The $NaAlCl_4$ electrolyte was prepared by mixing anhydrous $AlCl_3$ (from Fluka) with analytical grade NaCl, dried at 175°C. The mixing and subsequent melting of the mixture were performed in a glove box purged with dry air (dew point < −55°C). Thereafter, the melt was pre-electrolyzed between aluminum electrodes (250 mA, 24 to 72 h) and filtered through a borosilicate glass filter. The purified melt was almost water clear. Further purification was performed by zone refining in sealed ampuls.

Two "$NaAlSCl_2$"/$NaAlCl_4$ mixtures, used as sources of sulfide, were produced from $NaAlCl_4$ (zone refined), NaCl (purified in the molten state by HCl and filtered), Al (99.999%) and S (Riedel-de Haën 99.5%, further distilled twice), by means of the reaction 1b. The synthesis was carried out at 215°C in an evacuated ampul in a rocking furnace over a period of four days. A surplus of $NaAlCl_4$ was used giving mixtures with "$NaAlSCl_2$":$NaAlCl_4$ molar ratios of $1:7.97_5$ and $1:10.00_0$. The two mixtures were used in sulfide cells I and II, respectively, see below. Similarly, a "$NaAlSeCl_2$"/$NaAlCl_4$ mixture, with a molar ratio of $1:8.37_3$, was produced from $NaAlCl_4$ (pre-electrolyzed), NaCl (analytical grade and dried at 175°C), Al (99.999%), and Se (99.999% Koch-Light Laboratories, Limited).

The hygroscopic chemicals were stored in sealed Pyrex ampuls between uses.

Cycling experiments.—Cycling experiments were performed on cells shown in Fig. 1a. The electrolyte was pre-electrolyzed $NaAlCl_4$ saturated with a surplus of NaCl. The melting point of this electrolyte was 155.4_7°C, which should be compared with the value of 155.9_0°C obtained for an extrapolated oxide-free NaCl saturated melt.[5] The melting point depression corresponds to an oxide impurity content of ~0.045 mol/kg.

The nickel felt, of ~0.3 mm thickness, was cut to 1 × 3 cm^2 (weight *ca.* 200 mg) and spot welded to the tungsten wire.

Four cells were filled with electrolyte (each ~25.0 g or 14.7 ml at 175°C) in the dry air glove box. To three of the cells a further addition was made of either sulfur (Riedel-de Haën 99.5%, further distilled twice), selenium (99.999% Koch-Light Laboratories, Limited), or tellurium (Fluka, puriss.).

Finally, the cells were evacuated, sealed off, and placed in a holder in a home-made oven heated to 175°C by circulated air.[2]

The charge/discharge cyclings were performed by means of a microprocessor controlled battery test equipment.[2]

Raman spectroscopy.—Two types of cells shown in Fig. 2 were used, shaped to fit the Raman spectroscopy furnace and to allow electrolyte changes during cycling to be observed spectroscopically. An experimental difficulty with type (a) proved to be electrical short circuit due to dendrite formation. This problem was avoided with cells of type (b) due to the greater distance between the electrodes. The charging and discharging with type (b) needed to be performed outside the Raman furnace (the cell was too big to fit into the furnace). After each charge/discharge step, the electrolyte was frozen and the cell turned upside down. Part of the electrolyte could now be remelted in a flame and the melt allowed to run down in the cuvette section (G) which was then introduced in the Raman furnace. In this way spectra were obtained of the electrolyte before and after each charging or discharging step.

Potentiometric measurements.—Potentiometric measurements were performed by means of three-chamber cells, see Fig. 1b. The chamber containing an aluminum reference electrode was connected to anode and cathode chambers through porous ceramic Al_2O_3 pins (6 mm length, 1.2 mm diam, and pore size 1.7 to 1.8 μm). Four cells were investigated containing either no chalcogenide, dissolved sulfide (two cells), or selenide, respectively.

The masses of nickel felt and electrolyte used in these cells are given in Table I. Five layers of nickel felt, with a geometrical surface area of 1.9 × 1.0 cm^2, were tied together and pinned to the tungsten current collector by means of a nickel wire (3.5 cm length, 0.5 mm diam) giving a geometrical electrode thickness of 1.5 mm (sulfur cell II had four layers and was thinner). The given size and mass of the electrodes corresponds to a porosity of about 75-85 volume percent (v/o).

The cells were loaded with chemicals in an argon-filled glove box (Vacuum Atmospheres, Corporation). Sulfide and selenide were added in the form of the intimate mixtures of $NaAlCl_4$ and "$NaAlSCl_2$" or "$NaAlSeCl_2$," as described above. The solvent was made slightly acidic [~0.51 mole percent (m/o) $AlCl_3$] to make possible a variation in the chloride activity or equivalently, the aluminum electrode potential. This is essential to derive conclusive information from the potentiometric measurements. On the contrary, in the cycling experiments and Raman studies, the solvent was $NaAlCl_4$ saturated with NaCl.

After filling, the cells were evacuated and all loading tubes sealed off under vacuum. Subsequently the pressure equilibration tube, between reference and anode chambers (A, Fig. 1b) was closed in order to prevent distillation of $AlCl_3$ from the anode/cathode compartments to the reference compartment. The cells were then placed in a regulated furnace at 175.0 ± 0.3°C. The furnace was kept continuously rocking during the experiments to ensure fast electrolyte equilibration in the anode/cathode chambers and a constant reference potential.

Aluminum anode and nickel felt cathode potentials were measured relative to the reference electrode by means of a xt-recorder with relative accuracy better than ±0.5 and ±1.0 mV for anode and cathode, respectively (absolute accuracies are estimated to be better than ±1.0 and ±2.0 mV). Voltage calibration was repeatedly done with a digital multimeter.

To allow for measurements of equilibrium potentials, charging and discharging were performed in successive steps, consisting of a galvanostatic period (lasting from 1 to 4 h) followed by a rest period, lasting between 12 and 24 h, depending on how fast the cells equilibrated. The cells normally reached constant anode and cathode potentials

Table I. Chemicals loaded into the anode/cathode compartments of the cells used for potentiometric measurements and calculated molar compositions. The reference compartments contained $NaAlCl_4$ saturated with NaCl.[a]

Cell type	Weighed chemicals in gram				Corresponding mol compositions		
	Ni-felt	$NaAlCl_4$	"$NaAlXCl_2$"[b] + $NaAlCl_4$	$AlCl_3$[c]	n_{NaCl}	n_{AlCl_3}	$n_{Al_2X_2}$[b]
No chalcogen	0.546_5	25.01_1	0	0.56_8	0.1304_1	0.1346_7	0
Sulfur (cell I)	0.506_9	19.72_3	2.08_5[d]	0.63_6	0.1139_8	0.1179_0	$4.13_1 \cdot 10^{-4}$
(cell II)	0.388_0	20.11_0	2.49_9[d]	0.50_7	0.1169_2	0.1211_2	$4.02_3 \cdot 10^{-4}$
Selenium	0.570_1	21.19_7	2.70_6[d]	0.53_6	0.1245_7	0.1275_9	$4.99_5 \cdot 10^{-4}$

[a] *Ca.* 11 g $NaAlCl_4$ and *ca.* 2 g NaCl.
[b] X = S or Se.
[c] Distilled twice and recrystallized.
[d] The composition of the mixture is given in the Experimental section.

(within ±0.5 and ±1.0 mV, respectively, over a period of at least 2 h) in less than 12 h. These potentials were taken to be equal to the equilibrium values. In the case of selenide, especially near the end of discharging, equilibrium was not reached even after 24 h.

Constant current of either ~1 or ~2 mA was used during the galvanostatic periods. The exact value was measured by means of a 0.05% 10 Ω resistance and a Keithley 175 digital multimeter. Due to small current fluctuations the accuracy of given charges was *ca.* ±2.5%.

Results

Charge/discharge behavior of the different battery cells.—A selected number of cycles obtained with the four cells A, B, C, and D, containing no chalcogen at all, sulfide, selenide, and telluride, respectively, are shown in Fig. 3. Charging and discharging of cell A proceeds mainly at a single voltage level or plateau, associated with formation/decomposition of $NiCl_2$. The charge/discharge curves of the chalcogen containing cells (C, B, and D) differ markedly from those of cell A, showing that the chalcogens are chemically active in the cathode reactions. Compared with the chalcogenide free cell, those containing chalcogen showed improvements with regard to rate capability.

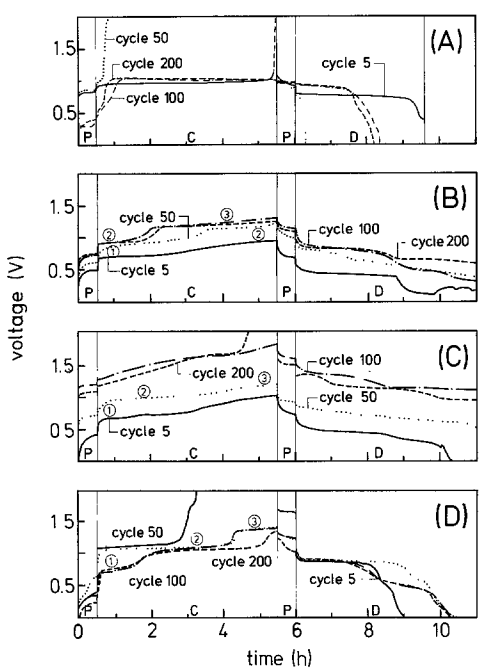

Fig. 3. Constant current charge/discharge curves for cycles No. 5, 50, 100, and 200 of the battery cells at 175°C. (A) Cell without additions to the $NaCl_{sat}$-$AlCl_3$ electrolyte (with 50.2 m/o NaCl); (B) cell with 0.387 mol S per liter; (C) cell with 0.376 mol Se per liter; (D) cell with ≤0.027 mol Te per liter. Applied charging and discharging currents were 5 ± 5% mA, except for cell A, where 1 ± 5% mA were used after cycle No. 64. Charging and discharging were followed by a pause of 0.5 h. Termination conditions were for charging a maximum charging time of 5 h and a maximum voltage of 2.0 V, and for discharging a maximum charging time of 5 h and a minimum voltage of 0.0 V, except for cell A, where the minimum voltage was 0.4 V for cycle No. 1-64 and 0.1 V for cycle No. 65-200. Notation: P, pause; C, charging; D, discharging. Plateaus are labeled No. 1, No. 2, and No. 3, according to the description in the text.

Since the accuracy of the applied currents were ±5%, charging and discharging currents may have deviated up to ±10%. Therefore, the relatively poor coulomb efficiency of cells A and D(Te) may be due to higher discharging than charging currents during cycling. Similarly, the gradual increase of charging and discharging voltage with increasing number of cycles, observed for cells B(S) and C(Se), was probably caused by cycling with higher charging than discharging currents.

The charge/discharge curves in Fig. 3B are very similar to the ones found in experiments with cathodes prepared from nickel sulfides.[2] At least three horizontal plateaus, labeled No. 1, No. 2, and No. 3, are seen in Fig. 3B. Also in the telluride system (Fig. 3D), three plateaus are observed (most clearly seen from the charging curves), situated at about the same potentials as those in the sulfide system. At least the two lowest plateaus are also present in the selenide system (barely perceptible from the charge curves of cycle 5 and 50, respectively, see Fig. 3C). This indicates that similar reactions may take place in all three chalcogenide systems. As shown in Part I[1] plateau No. 1 involves formation/decomposition of essentially Ni_yS_z in the sulfide system, and Ni_ySe_z in the selenide system. The intermediate plateau, No. 2, of sulfide containing cells at ~0.975 V is associated with $NiCl_2$, or a $Ni_yS_zCl_{2y-2z}$-type compound with $y > (4.4 \pm 0.2) \cdot z$, see below. Accordingly, the voltage of plateau No. 2 for chalcogen containing cells corresponds closely to the voltage observed for cell A. Plateau No. 2 appears most clearly on Fig. 3D probably because tellurium was not added in excess (50 mg of Te were added corresponding to 35 mg Ni or 85 mg Ni_3Te_2) and probably only part of it went into solution. Since plateau No. 3 at ~1.2 V (seen clearly from the charge curves of cells B and D) was not observed for the chalcogenide free cell (A), the reaction taking place along plateau No. 3 must involve a compound containing chalcogen. It probably contains higher oxidation states of nickel or sulfur, since a plain nickel (II) chalcogenide is expected to give a lower potential than $NiCl_2$.

Compared with the sulfide and telluride systems, the charge/discharge curves obtained with selenide show a smoother appearance, probably due to inferior cathode reaction kinetics. This together with a high state of charge may explain the obtained high cell voltages.

Chalcogen participation in cathode reaction.—The experiments discussed in the following were performed in order to examine the sulfur and selenium cell reactions in more detail. The identification of nickel sulfide phases by postoperation x-ray powder diffraction on cathode material from type B batteries proved to be not easily done. Many overlapping lines were observed from samples covered by 6 μm Al foil protecting against moisture. However,

lines indicative of Ni_3S_2 and perhaps NiS and $NiCl_2$ were observed.[6] Experiments aimed at finding a procedure to remove surplus melt without also decomposing the nickel sulfide have so far been unsuccessful.

In the literature,[7] the positive effect of adding sulfur to nickel powder cathodes in pure $NaAlCl_4$, has been attributed to morphological changes, in which sulfur and sulfide seemed to inhibit nickel grain growth.

Gravimetric analysis of sulfur.—The electrolytes from three fully charged battery cells (with cathodes originally prepared from nickel mesh and nickel sulfide and with sulfide-free $NaAlCl_4$ electrolyte and cycled more than 100 times) were filtered and analyzed chemically for sulfide. The analysis, performed by oxidizing sulfide to sulfate and precipitating it as $BaSO_4$, showed little sulfur (only 1.6 ± 1.9% of the total amount was present in the electrolyte). Therefore, practically all sulfur must be contained in the cathode of fully charged cells. The question was then to show that sulfur is exchanged between cathode and electrolyte during cycling.

Raman spectroscopy.—This technique was applied in order to measure the changes in concentrations of sulfide and selenide in the electrolyte during charging and discharging. We first recorded the reference spectra shown in Fig. 4. Figure 4A is a spectrum of pure zone refined $NaAlCl_4$. Figure 4B shows a spectrum of $NaAlCl_4$ saturated with NaCl and containing 0.9 F of sulfide (the formality, F, is defined as the initially weighed molar amounts divided by the volume of the molten mixtures in liters). The shoulder bands located at ~333 and ~304 cm^{-1} have been assigned to the two different kinds of sulfide species, —Al—S—Al— and

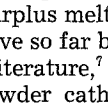

respectively.[8] In Fig. 4C is shown the Raman spectrum of $NaAlCl_4$ saturated with NaCl and containing 0.9 F selenide. The band located at *ca.* 290 cm^{-1} has been seen in the analogous $CsCl\text{-}AlCl_3$ system (located at *ca.* 287 cm^{-1}) and has been assigned to —Al—Se—Al— species present in the electrolyte.[8]

Figure 5(A) shows the Raman spectrum of a battery electrolyte shortly after all elemental sulfur had reacted via Eq. 1a with $NaAlCl_4$ and NaCl (added in excess). A strong fluorescence from such samples unfortunately always gives a low signal-to-noise ratio in the spectrum. The sulfide concentration should be around 0.6 F, but the absence of a shoulder at 333 cm^{-1} in Fig. 5(A) seems to indicate less sulfide. Presumably this means, that a part of the added sulfur had reacted with nickel instead, forming insoluble nickel sulfide at the cathode. After introductory charging of the cell (corresponding to a ~7% decrease of theoretical formality, calculated on basis of the added divalent sulfur) a spectrum such as Fig. 5(B) was obtained. The fluorescence had disappeared and no sign of sulfide in the electrolyte can be seen; the sulfide must be on the Ni electrode. The cell was then discharged and charged several times and finally it was discharged through a 10 Ω resistor until the current vanished. Raman spectra of the resulting "dis-

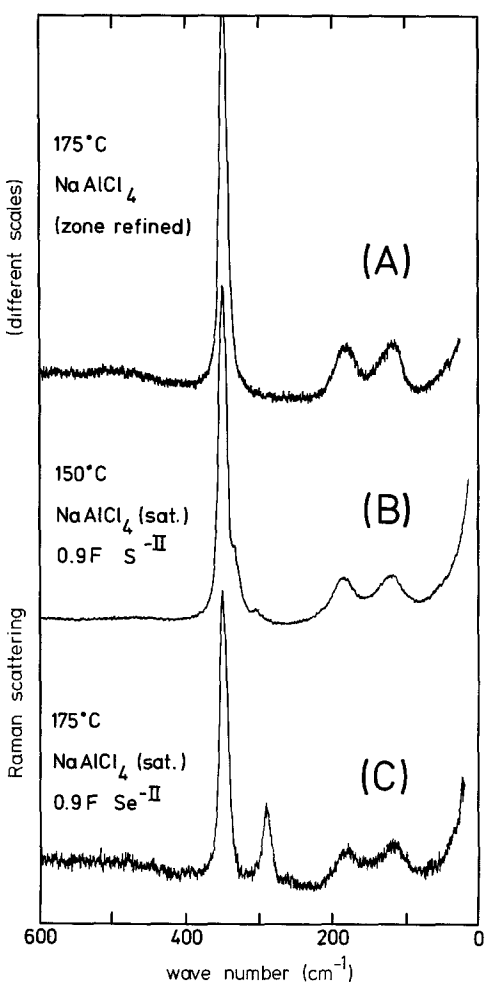

Fig. 4. Raman spectra of $NaAlCl_4$ melts. (A) Pure zone refined $NaAlCl_4$. (B) $NaAlCl_4$ (sat.) with 0.9 F S^{2-} (produced by reaction between aluminum and sulfur). (C) $NaAlCl_4$ (sat.) with 0.9 F Se^{2-} (produced by reaction between aluminum and selenium).

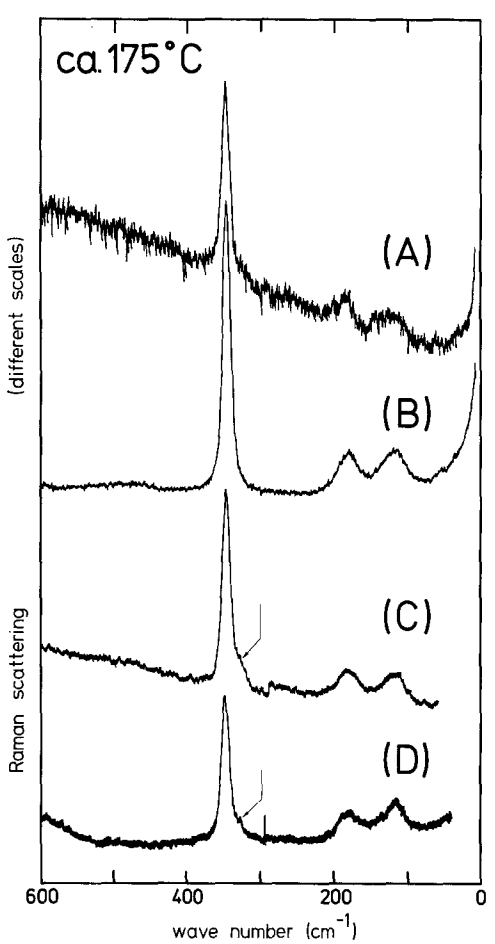

Fig. 5. Raman spectra of the electrolyte with 0.6 F S^{2-} of a cell containing nickel felt in excess. (A) Spectrum obtained shortly after equilibration of $NaAlCl_4$, NaCl, and sulfur. (B) Spectrum obtained after charging the cell corresponding to *ca.* 7% of the theoretical amount (calculated on the basis of added sulfur). (C) and (D) spectra obtained after having cycled the cell several times and finally short-circuiting it.

charged" electrolyte [see Fig. 5(C) and (D)] showed that sulfide was now present in the melt. The returned fluorescence made it difficult to read an accurate value of the concentration of sulfide from the given spectra; it is probably not much less than the expected 0.6 F.

In the next series of Raman experiments we examined the effect of selenide in a battery cell. Due to the stronger and better located selenide band [at *ca.* 290 cm^{-1}, Fig. 4(C)], it was easier to estimate the selenide concentrations.

Figure 6 shows a plot of the Raman results obtained with the cells of type (a) and (b), see Fig. 2. Since different starting concentrations of selenide were used, the plot was constructed using concentration ratios and coulomb ratios. The concentration ratio is the ratio of the scattering intensity of the selenide band at 290 cm^{-1} relative to the $AlCl_4^-$ main band, normalized to 1. The coulomb ratio (degree of charge) is the number of coulombs passed through the cell relative to the calculated capacity based on the amount of divalent selenium present in the cell. In order to determine the concentration ratios, about seven Raman spectra were recorded for each run and the average and the standard error determined.

From Fig. 6 it is clear that selenium reacts quantitatively in the form of Se^{2-} with the nickel felt electrode, probably forming a Ni_ySe_z compound.

The next step was to see what happened during discharging. Here only cell type (b) was used, and in a more elaborate way. After the first charging of the cell, it was turned upside down and the electrolyte allowed to run down in the bulb (D). The bulb was then removed (broken off in a glove box) and new-zone-refined electrolyte without selenide added to the cell which was then sealed again. In this way the electrolyte contained very little selenide before discharging.

The result of the first discharging is shown in Fig. 7. In the beginning the amount of selenide seems to follow the diagonal line but after a while the curve levels off, indicating a gradual shift in reaction mechanism. As shown below the shift most probably involves the compounds Ni_ySe_z and $Al_vNi_ySe_z$. The fact, that only about half of the selenide dissolves in the electrolyte can be explained by slow reaction kinetics and relatively fast discharge rate.

Potentiometric Results

The experimental data from the potentiometric investigations are analyzed by comparing with theoretical model calculations of the system Al/NaCl-$AlCl_3$-Al_2X_3/Ni (X = S, Se, Te) and the corresponding system without chalcogen. The developed model was present in Part I.[1]

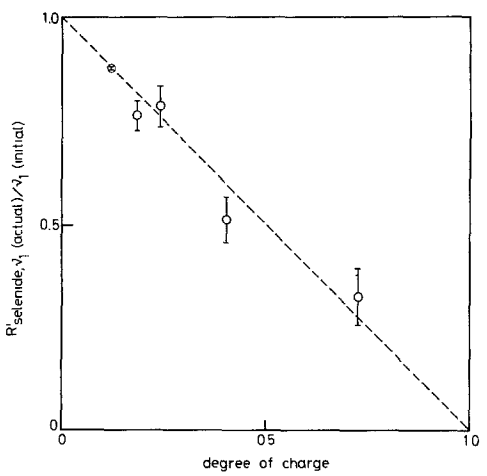

Fig. 6. Variation of the relative Raman scattering intensity of the selenide band of the battery electrolytes of NaCl-saturated Al/NaCl-$AlCl_3$-Al_2Se_3/Ni-felt cells during first charging as a function of the degree of charge.

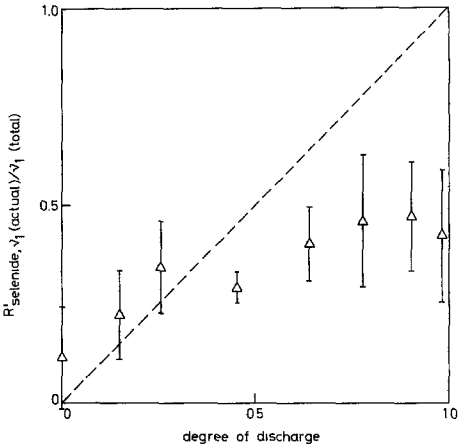

Fig. 7. Variation of the relative Raman scattering intensity of the selenide bands of the battery electrolytes of initially charged NaCl saturated Al/NaCl-$AlCl_3$-Al_2Se_3/Ni-felt cells during first discharging as a function of the degree of discharge.

The Chalcogenide-Free Cell

The variation of the cathode potential and cell voltage during first charging and discharging is shown in Fig. 8, whereas the corresponding variation of the anode potential is given in Fig. 9 together with model calculations. The experimental data points in the two figures belong together in the sense that for every value of the cathode potential or cell voltage an equivalent value (with identical abscissa) exists for the anode potential and vice versa. The same will hold later on for corresponding figures showing sulfide and selenide results. The discontinuity in the charging curves of Fig. 8 and 9 was due to an unintended partly discharging of the cell (with about 200 to 450 coulombs, as estimated from Fig. 9, see arrow), which occurred during reheating of the cell after a stop in charging and solidification of the electrolyte. More coulombs could be passed through the cell during the second part of charging than lost during the unintended stop, indicating that repeated cycling improves the electrode performance by modifying its physical structure.

It appears from Fig. 8 and 9 that both the anode and cathode potentials decrease during charging, however, the anode potential with a higher rate causing the cell voltage to slightly increase. These observations are in agreement with the course of the calculated curves, shown in Part I, Fig. 2, because the electrode reactions cause a decrease in the mole fraction of $AlCl_3$ due to deposition of aluminum at the anode.

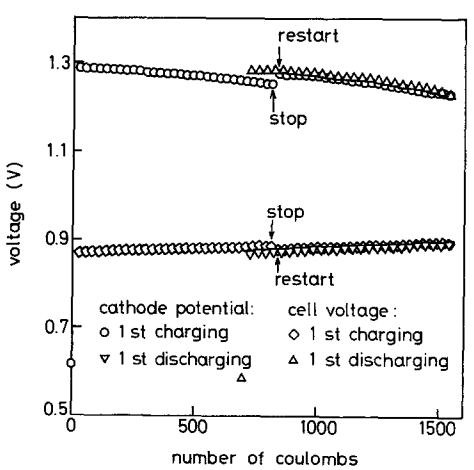

Fig. 8. Measured equilibrium values at 175°C of nickel cathode potential and cell voltage *vs.* number of coulombs, of a Al/NaCl-$AlCl_3$/Ni-felt cell; electrolyte composition varied between 0.502-0.508 m/o $AlCl_3$.

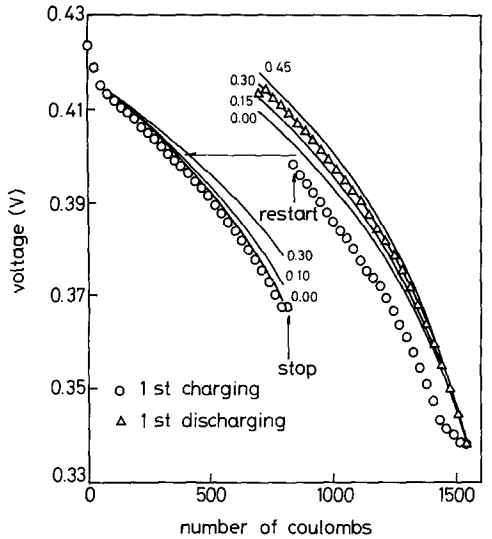

Fig. 9. Measured aluminum anode potential points at 175°C belonging to the nickel potentials in Fig. 8. The solid lines shown are model calculations in accordance with Eq. 11 and 16 in Part I for charging and discharging, respectively. The stated labels designate the amount of NaCl "consumed" per six electrons transferred.

It is seen from Fig. 9 that the decrease of the anode potential was faster at the beginning than during the main part of charging. A similar effect was observed in the case of the sulfide and selenide containing cells. An explanation may be that impurities take part in the electrode reactions and are gradually consumed during the first coulometric titration steps. The change of the cathode potential from 0.618 to 1.288 V, as a result of the first step, reflects a change in the cathode reaction, which too may affect the variation of the anode potential.

Overcharge reaction.—There is strong evidence that an overcharge reaction, with generation of Cl_2 at the cathode, took place during the last titration period before the unintended stop and during the last four titration periods before discharging (in the second part of charging). The cathode overvoltage (at an applied current of 2 mA) changes from ~100 mV, during titration in the main part of charge, to ~1.25 V during overcharge, assuming negligible overvoltages associated with transport of ions in the bulk electrolyte. The anode overvoltage remained unchanged at ~10 mV. The nonequilibrium cathode potential was 2.5 V. A potential plateau at that level has been found by other investigators.[9-11] The associated reaction most likely proceeds according to

$$4AlCl_4^- \rightarrow 2Al_2Cl_7^- + Cl_2 + 2e^- \quad [2]$$

causing decomposition of the electrolyte and evolution of Cl_2. Generated Cl_2 dissolves to some extent in the melt. According to Wærnes and Østvold[12] the solubility of Cl_2 in an acidic NaCl-$AlCl_3$ melt with X_{AlCl_3} = 0,51 at 175°C is $9 \cdot 10^{-6}$ mol cm^{-3} at 1 atm Cl_2 pressure. Reduction of dissolved Cl_2 is possible either at the cathode or anode and may proceed via the following reactions

$$\text{Cathode:} \quad Cl_2 + Ni \rightarrow NiCl_2 \quad [3]$$

$$\text{Anode:} \quad 3Cl_2 + 2Al \rightarrow 2AlCl_3 \quad [4]$$

The reversible overcharge reaction with generation of Cl_2 at the cathode and reduction of Cl_2 at the anode is a very favorable inherent property of the present battery system.

Modeling of the experimental results.—Charge reaction.—The solid lines in Fig. 9 are calculated curves fitted to the course of the anode potential. During charging, the curves were calculated according to Eq. 11 (Part I), corresponding to formation of a general $Na_xNi_yCl_{2y+x}$ compound containing divalent nickel. However, the curves depend only on the relative consumption of $AlCl_3$ and NaCl.

As stated in Part I, formation of an Ni(I)-compound is not likely. Moreover, the number of coulombs passed through the cells correspond to more nickel than present in the cells if Ni(I) alone was formed.

The first three measured anode potentials were not included in the model fitting in order to obtain good agreement with experiment and theory. The model potential curves were forced to start at the fourth data point (0.4134 V), by using, as initial conditions, 0.1343_8 mol $AlCl_3$ and 0.1301_5 mol NaCl. In all model calculations throughout this paper, initial moles of $AlCl_3$ were calculated from the weighed out amount of $AlCl_3$ and corrected for the net consumption of $AlCl_3$, whereas initial moles of NaCl were calculated by means of the model so that the initial anode potential became equal to the experimental value.

Three curves are shown in Fig. 9, corresponding to different values of the fitting parameter, $3 \cdot x/y$, see Eq. 11, Part I. The best fit is obtained for $x = 0.0$, which corresponds to formation of $NiCl_2$. No attempt was made on fitting to the second part of the anode charging curve.

Precision.—To estimate the accuracy of the model, we performed several calculations, assuming somewhat different starting values. As a result, $3x/y$ is probably contained in the interval $0 \leq 3x/y < 0.05$ with a high degree of certainty (the lower boundary is due to physical reasons).

One further source of error has been considered. Due to different composition of the electrolyte in the reference and cell compartments, some net diffusion of ions might occur through the porous separator. This should show up as a steady increase of the deviation between the experimental data and model curves in Fig. 9. Such an effect was not seen, even though 25 days expired during charging with the first 800 coulombs. Also, during an open-circuit experiment, lasting for about one week, no appreciable drift of the anode potential was observed. Therefore, diffusion of ions through the separator can be assumed negligible. This was valid too for the cells with sulfide and selenide.

Discharge reaction.—A general discharge reaction is given in Eq. 16, Part I. Reduction of $NiCl_2$ to Ni is assumed to be accompanied with consumption of NaCl at the cathode and formation of intermediate $Na_xNi_yCl_{2y+x}$-compounds.

The discharge curve of the anode is shown in Fig. 9 together with 4 theoretical curves, all starting from the potential 0.3382 V and calculated in accordance with reaction 16, Part I. The initial conditions used for the model curves were 0.1290_6 mol of NaCl and 0.1300_4 mol of $AlCl_3$ ($AlCl_3$ was corrected for the coulombs lost by overcharging and during the stop, ~120 and ~200 coulombs, respectively). The inaccuracy of the initial amount of $AlCl_3$ is therefore relatively large. However, model calculations show that this only affects the theoretical curves slightly, as a consequence of the fact that the number of coulombs passed through the cell during charging only corresponds to a small part (~5%) of the total amount of $AlCl_3$ present in the electrolyte. The curve for $x = 0.3$ represents a good fit to the experimental data, whereas curves for $x = 0.15$ and $x = 0.45$ state the margin of error of the model calculations. The lowermost curve gives the expected variation of the anode potential if no NaCl was "consumed" during discharging at all. The deviation from the experimental data can hardly be explained by error sources. Hence it is concluded that sodium takes part in the cathode reaction and is consumed during discharging. The "consumed" NaCl probably exists in the cathode in the form of NaCl particles physically isolated from the acidic melt.

The $NiCl_2$/Ni electrode is known to be fully reversible in basic $NaAlCl_4$ melts.[13] In contrast to this we obtained a coulomb efficiency of only 70 to 85% for the first cycle. One reason might be that $NiCl_2$ is slightly soluble in acidic $NaAlCl_4$. Another factor contributing to low coulomb efficiency is shedding of cathode material. Visual inspection of the cell after the first cycle revealed deposition of a small amount of black material at the bottom of the cathode compartment. Considering the high utilization of nickel (about

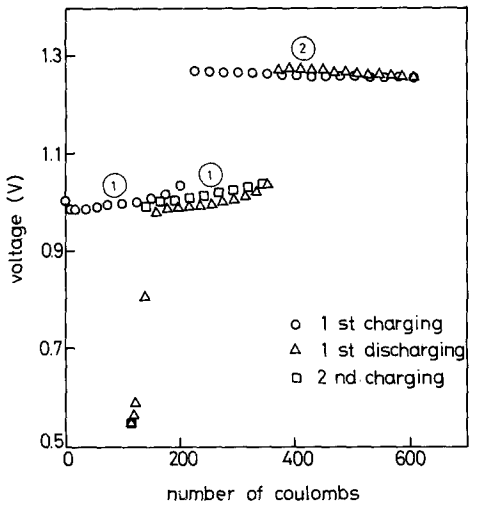

Fig. 10. Measured equilibrium potentials at 175°C of the nickel cathode *vs.* number of coulombs, of the Al/NaCl-$AlCl_3$-Al_2S_3/Ni-felt cell I, see Table I. Potentials are measured relative to an Al/$NaAlCl_4$ reference electrode saturated with NaCl. Plateaus No. 1 and No. 2 are indicated.

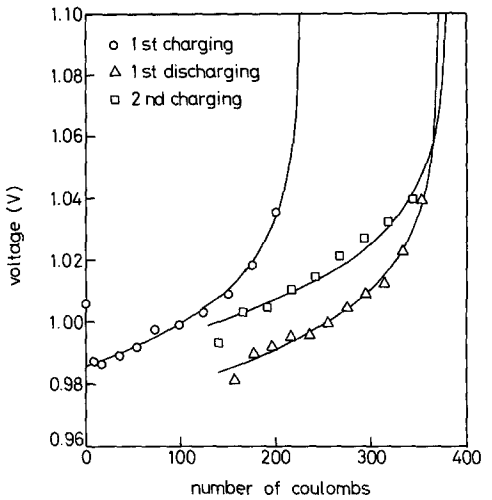

Fig. 12. Measured cathode potential points from plateau No. 1, Fig. 10, fitted by calculated potential curves belonging to the sulfide species $Al_2SCl_5^-$, (*n*, *m*) = (2, 1).

50 to 60% during first charging), the constant disturbances caused by the rocking, and the lack of mechanical support, the structural integrity of the cathodes is surprisingly good.

Variation of the cathode potential.—The variation of cathode potential *vs.* melt composition was analyzed in Part I. A plot of the experimental data as $\{E_C \cdot F/(R \cdot T \cdot \ln 10) - g/6 \log([Na^+][Cl^-])\}$ *vs.* $pCl = -\log [Cl^-]$ in Fig. 3, Part I, demonstrates a linear dependence with a slope close to +1. This means that the observed variation of the cathode potential can be explained solely by changes in the electrolyte. For sake of clarity, only those experimental data used for curve fitting in Fig. 9 were included in Fig. 3.

The consumption of NaCl was also determined from the variation of the cathode potential by depicting the experimental data as $E_C \cdot F/(R \cdot T \cdot \log 10) + \log [Cl^-]$ *vs.* $\log([Na^+] \cdot [Cl^-])$. The results were in reasonably good agreement with the NaCl-consumption obtained from model fitting to the anode potential curve, see Part I.

The Sulfide Containing Cells

Two cells (I and II) were investigated, see Table I. For cell I the variation of the equilibrium potentials of cathode and anode *vs.* the number of coulombs passed through the cell are shown in Fig. 10 and 11, respectively.

The course of the cathode potential reveals two plateaus, No. 1 and No. 2, indicating that two sequential cathode reactions are taking place during both charging and discharging. As seen from Fig. 11, the shift between the two charge/discharge reactions is associated with a change in the variation of the anode potential, which too reflects that two different cathode reactions are involved.

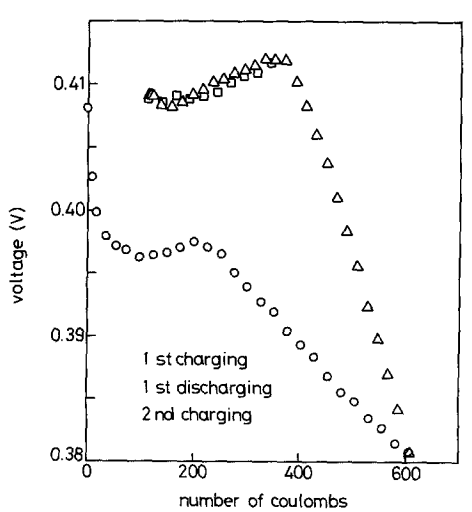

Fig. 11. Measured equilibrium aluminum anode potentials of cell I, belonging to the cathode potentials shown in Fig. 10.

The low potential plateau.—Plateau length.—Since plateau No. 1 is not observed for the chalcogenide-free cell, it is obviously due to formation/decomposition of (in general) a $Na_xNi_yS_zCl_w$ compound. The corresponding overall cell reaction and the associated changes in the composition of the electrolyte are given in Part I, by Eq. 22 and 23, respectively.[1]

Assuming sulfide to react quantitatively with the nickel felt electrode (the formed compound may still contain Na and Cl), the length of plateau No. 1 should be ~239 coulombs, calculated from the weighed amount of sulfide. Experimentally, 225, 212, and 240 coulombs (read from Fig. 12, see above) were obtained for first charging, first discharging, and second charging, respectively. The deviation of these numbers from 239 coulomb may be due to inaccuracy in the measured charge and the amount of sulfide. Furthermore, the relatively short plateau-length of the first discharging (212 C) and long one of the second charging (240 C) are the result of slow cathode processes taking place below ~0.9 V (cathode potentials given for this range are not true equilibrium values).

Thus, the length of plateau No. 1 is in close accordance with sulfide reacting as S^{2-}. Furthermore, the anode potential is essentially constant along plateau No. 1, see Fig. 11. These two experimental results were compared in Part I with Eq. 23, which gave quantitative evidence that plateau No. 1 is associated with formation/decomposition of essentially a pure nickel sulfide. Most probably Ni_3S_2 is formed since this compound has been identified by means of x-ray diffraction on one of our cathodes[6] and also in nearly discharged $NaAlCl_4/NiS_2$-cathodes after removal of $NaAlCl_4$ by washing with CH_3CN.[9]

Cathode plateau-curve form.—The dependence of the cathode potential of plateau No. 1 on melt composition was given in Part I by Eq. 27. Based on this expression cathode potentials were calculated *vs.* number of coulombs for different assumed sulfide species $Al_nS_{n-1}Cl_{2n+2-m}^{(n-m)-}$ designated by (*n*, *m*). The results are given in Fig. 4, Part I.

The calculated potentials belonging to the sulfide species (2, 1), , are fitted to the experimental cathode potential points in Fig. 12, which is an enlarged cutout of Fig. 10. Among the potential-curves from Fig. 4 only the one for the sulfide species (2, 1) agrees well with the experimental data. The second best fit is obtained by the (3, 2)-curve. This strongly indicates, that dissolved

sulfide preferably exists in the form of sulfide-chloride double bridges in molten acidic NaCl-$AlCl_3$, at least for compositions greater than *ca.* 0.505 m/o $AlCl_3$. The same result was obtained previously by means of Raman spectroscopy.[8] We were unable in that work to estimate n and m (apart from $m > 0$) of the $Al_nS_{n-1}Cl_{2n+2-m}^{(n-m)-}$ type species, in acidic melts. For basic melts generally $m = 0$. In dilute basic solutions n seems to attain small values like 3 to 4, whereas in more concentrated melts higher values of n are reached. The $n = 2$-type species was found to be of minor importance. This may also be valid in the bulk electrolyte of acidic melts. On the other hand, at the electrode the sulfide species $Al_2SCl_5^-$ ($n = 2$, $m = 1$) seems to be dominating, since only this species provides a good description of the variation of the cathode potential (species entering into the Nernst equation are those staying at or close to the electrolyte/electrode interface). The cathode reaction itself may contribute to the formation of sulfide species with small chain lengths. If sulfide is released to the melt most likely a small ion ($n = 2$) is formed. On the other hand, if a sulfide species reacts with a nickel atom the reacting species will lose one monomeric unit or it will break into two parts if either an end sulfide atom or a sulfide atom in the middle of the chain is captured, respectively. A requirement for the existence of small sulfide species (n small) nearby the electrode is that the cathode reaction is fast (associated with a high exchange current density) compared with the polymerization reaction of the sulfide species.

Anode plateau-curve form.—Figure 13 shows the variation of the anode potential during the low potential plateau, No. 1, for first discharging and second charging, together with calculated curves for different assumed sulfide species (n, m). The increase in the measured anode potentials *vs.* number of coulombs shows, that the chloride concentration decreases (see Part I, Eq. 13) as sulfide in the electrolyte is "consumed" by the cathode reaction. This course is expected if sulfide mainly exist as sulfide-chloride double bridges of the type 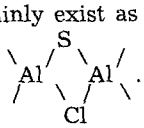 . Release of sulfide from this configuration causes consumption of almost three free chloride ions, since aluminum prefers a four-fold coordination. Thus, consumption of three sulfide ions by the cathode reaction and the associated release of eight chloride ions at the anode (due to reduction of two $AlCl_4^-$) causes a net consumption of one chloride ion. On contrast, two extra chloride ions are produced for every net consumption of three sulfide atoms, when sulfide mainly exists in the form of 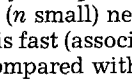 units. Therefore in Fig. 13, the calculated anode potentials belonging to sulfide species (2, 0) and (8, 0) to (8, 4) decrease and the other curves increase *vs.* number of coulombs. The uppermost model curve is obtained for the species (2, 0). At the other extreme, the slope of the model curves belonging to the species (n, m) = (n, $n-1$) increases slowly (with decreasing rate) as a function of increasing n, see the three lowermost curves in Fig. 13.

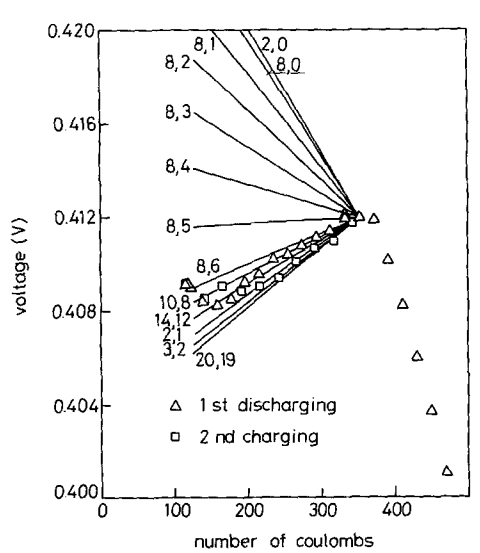

Fig. 13. Measured anode potential points from Fig. 11 and calculated anode potential curves belonging to different selected sulfide species of the type $Al_nS_{n-1}Cl_{2n+2-m}^{(n-m)-}$, designated by ($n$, m) in the figure.

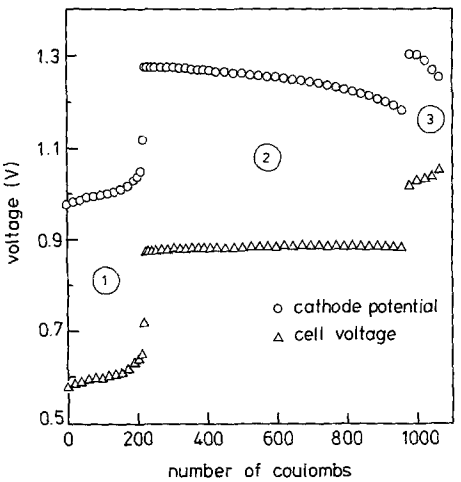

Fig. 14. Measured equilibrium values at 175°C of nickel cathode potential and cell voltage *vs.* number of coulombs of the Al/NaCl-$AlCl_3$-Al_2S_3/Ni-felt cell II, see Table I. Plateaus No. 1, No. 2, and No. 3 are indicated.

As seen, only model curves for sulfide species with relatively "large" values of m ($m = n - 1$, $m = n - 2$) fits well to the experimental anode potentials. For small values of n, reasonable good agreement with experiment is obtained, with the sulfide species (n, $n - 1$) = (7, 5), (8, 6), (9, 7), (10, 8), (11, 9), (12, 10), (13, 10), (13, 11), (14, 11), (14, 12), (15, 12), (15, 13), and so on. Thus, in acidic melts sulfide seems to exist mainly as sulfide-chloride double bridges, as found above from fitting to the cathode potential-curves. The eventual complication of a changing degree of polymerization *vs.* the sulfide concentration was left out of the model calculations. To summarize, only by assuming the sulfide species $Al_2SCl_5^-$ to be present in the melt nearby the electrode the observed variation of the cathode potential can be explained. On the other hand, in the bulk electrolyte sulfide may preferably exist in the form of polymeric species, *i.e.*, values of $n > 2$.

The high potential plateau, No. 2.—Along plateau No. 2, the level of the cathode potential and its variation *vs.* number of coulombs is very similar to the chalcogenide-free cell. The measured cathode potential points are ~5 mV lower compared with the calculated potentials of a Ni/$NiCl_2$-electrode, see Part I, Eq. 14. This small discrepancy between the experimental and calculated potentials, which can be explained by experimental inaccuracy and shortcomings of the model, strongly indicates that the formed compound has electrochemical properties very similar to $NiCl_2$ and certainly contains nickel in the divalent state. Therefore, generally the formed compound must belong to the series $Na_xNi_yS_zCl_{2y-2z+x}$. The stoichiometric coefficients cannot be determined very accurately from the data on cell I, since the exact length of plateau No. 2 is unknown. We shifted from first charging to first discharging before termination of plateau No. 2 in order to avoid any partly discharging of the cell caused by dendrites, compare results on the selenide cell below.

Cell II was investigated in order to identify the composition of the formed compound. To avoid the undesirable dischargings this cell was constructed in a way which differed slightly from cell I, see Fig. 1. In cell II the nickel felt was placed above the channel connecting the anode and cathode chambers, and the tungsten current collector in-

side the cathode chamber was "protected" by means of a glass tube.

The measured equilibrium potentials of cathode and anode and cell voltage are shown in Fig. 14 and 15 *vs.* number of coulombs. Charging was continued until plateau No. 3. Termination of the experiment occurred due to a power failure causing solidification of the electrolyte and cracking of the cell.

The general overall cell reaction taking place along plateau No. 2, assuming formation of $Na_xNi_yS_zCl_{2y-2z+x}$, is given in Eq. 28, Part I. Based on this equation, plateau No. 2 terminates when either all Ni-metal or all Ni_pS_z (presumably formed along plateau No. 1) is consumed. However, for the real electrode, plateau No. 2 may terminate before exhaustion of Ni-metal or Ni_pS_z since these compounds may become inaccessible by the electrochemical reaction with degree of charge. This may not be a real problem in the case of Ni_pS_z since it is formed on the surface of the Ni-felt. A lower limit for y/z can be derived by assuming termination of plateau No. 2 to be due to exhaustion of Ni_pS_z. According to Eq. 28 $3/(y - z)$ mol of $Na_xNi_yS_zCl_{2y-2z+x}$ are formed per 6 moles of electrons transferred, *i.e.* (mole of electrons)/(mole of $Na_xNi_yS_zCl_{2y-2z+x}$) = $2(y - z)$. This expression gives $y > (4.4 \pm 0.2) \cdot z$, utilizing (*i*) that the total amount of sulfide present in the cell was $(1.13 \pm 0.03) \cdot 10^{-3}$ mol (derived from the length of plateau No. 1 and (*ii*) that the length of plateau No. 2 was 760 ± 20 coulombs, see Fig. 14.

In Fig. 15 the experimental course of the anode potential is compared with calculated anode curves for different values of the parameters $3x/(y - z)$. Good agreement with experiment is obtained only if $x = 0$. From this result and the relation given above between y and z, it follows that plateau No. 2 is associated with a $Ni_yS_zCl_{2y-2z}$ compound with $y > (4.4 \pm 0.2) \cdot z$.

However, we cannot exclude the possibility that Ni_pS_z is inactive and pure $NiCl_2$ is formed, since the 980 coulombs passed through the cell until termination of plateau No. 2 corresponds to oxidation of at most $\sim 6.0 \cdot 10^{-3}$ mol of Ni-metal, which is still less than the total amount of Ni-felt $(6.61 \cdot 10^{-3}$ mol) in the cell.

The very large hysteresis between the anode potential curves along plateau No. 2 in Fig. 11 shows that sodium is "consumed" during the first discharging. Reduction of the compound formed during charging may take place via a sodium-chloride-rich phase, as discussed in Part I for chalcogenide-free cells. As seen from Fig. 10, essentially all loss of capacity occurs during the high potential range,

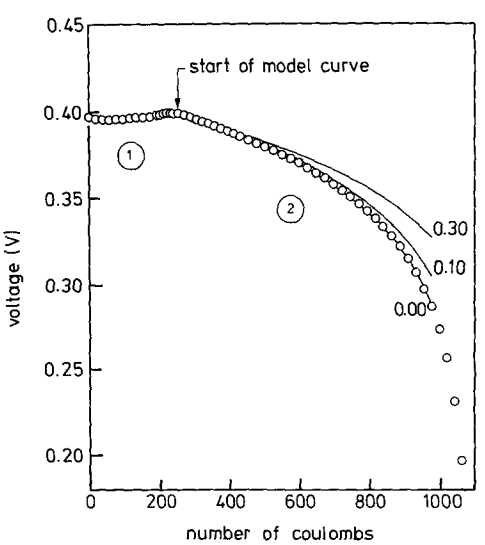

Fig. 15. Measured equilibrium aluminum anode potentials of cell II, belonging to the cathode potentials shown in Fig. 14. Solid curves were calculated based on reaction 28, Part I, assuming formation of $Na_xNi_yS_zCl_{2y-2z+x}$. The stated parameters are equal to $3x/(y - z)$.

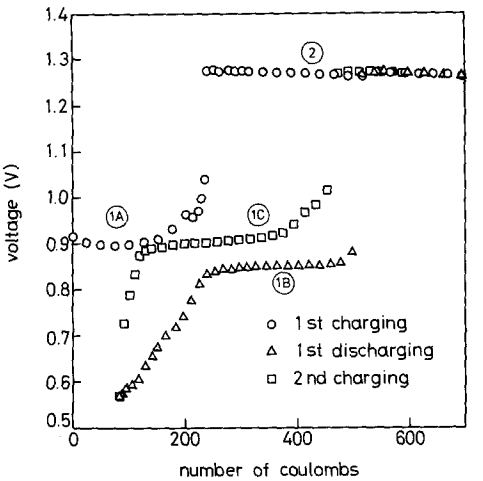

Fig. 16. Measured "equilibrium" potentials at 175°C of the nickel cathode of a Al/NaCl-$AlCl_3$-Al_2Se_3/Ni-felt cell *vs.* number of coulombs. Plateaus No. 1A, No. 1B, No. 1C, and No. 2 are indicated.

No. 2. Only minor changes in the length of the low potential plateau, No. 1 (which was ascribed to Ni_yS_z) were observed, indicating that essentially no sulfide was lost during cycling. This means, that unreacted cathode material must exist in form of $NiCl_2$, probably isolated from the current collector.

The Selenide Containing Cell

Measured potentials of the nickel felt cathode and aluminum anode are shown *vs.* number of coulombs in Fig. 16 and 17, respectively. The course of the potential curves of selenide and sulfide containing cells are qualitatively very similar, the only difference being a significant extra capacity beyond plateau No. 1 in the selenide case.

Cathode potentials below 1.2 V are not true equilibrium values, although 24 h, compared with ~14 h in the case of sulfide, were used as a rest period between each coulometric titration step.

The low potential plateau, No. 1.—Assuming a pure Ni_ySe_z-reaction the lengths of plateaus No. 1 should be ~290 coulombs, calculated from the amount of selenide. Read from Fig. 16, the experimental lengths of the plateaus No. 1A (first charging), No. 1B (first discharging), and No. 1C (second charging) are ~240, ~260, and ~330 coulombs, respectively. The deviation of ~17% of the length of plateau No. 1A from the calculated 290 coulombs can be explained by the slow cathode processes, inaccuracy in the measured charge and in the amount of selenide. Therefore, in accordance with what was found for sulfide, plateau

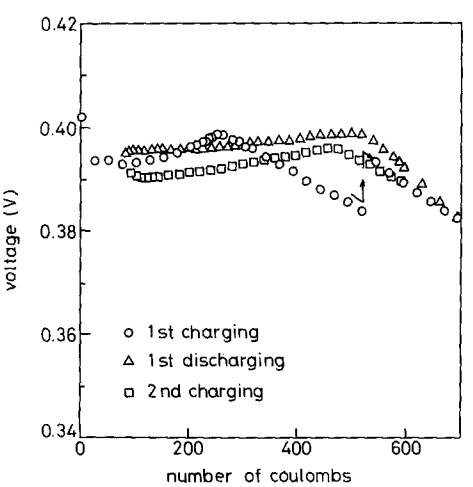

Fig. 17. Measured "equilibrium" aluminum anode potentials belonging to the cathode potentials shown in Fig. 16. For discontinuity see arrows and text.

No. 1A is most probably associated with a reaction involving Ni_ySe_z. This is the case also for the major part of plateaus No. 1B and No. 1C. However at the end of plateau No. 1B and particularly in the beginning of plateau No. 1C, the nickel selenide reaction is overlapped by the reaction taking place at potentials lower than those of plateau No. 1. Therefore, the length of the plateaus No. 1B and No. 1C are not comparable with the calculated 290 coulombs.

Model fitting to the low potential plateau, No. 1, has not been performed in the selenide case, since the measured cathode potentials below 1.2 V do not represent true equilibrium values.

Cathode reaction below potential plateau No. 1.—The variation in the concentration of selenide in the molten salt during discharging at potentials along and below plateau No. 1 (Fig. 16) was followed by Raman spectroscopy, see Fig. 7. It appears, that selenide in the cathode was released quantitatively during the first part of discharging, thereafter essentially no release of selenide occurred. This result indicates the existence of two consecutive cathode reactions in agreement with the measured curve for the cathode potential during discharging, as given in Fig. 16. Due to the Raman results decomposition of Ni_ySe_z and release of selenide to the melt must take place along plateau No. 1. As seen from the length of plateau No. 1B all selenide is released to the melt when the discharging is performed sufficiently slowly. That only about half of the selenide was released during the Raman measurements is due to the slow reaction kinetics in combination with the relatively fast discharge rate.

At potentials below plateau No. 1B a reaction given by Eq. 6 takes place due to the following reasons: The consumption of electrons at the cathode must be counterbalanced either by release of anions or by incorporation of cations into the electrode material. It cannot be the release of selenide nor the release of chloride since the cathode hardly contains significant amounts of these species. Therefore, the cations Na^+ and perhaps Al^{3+} have to enter the electrode material together with selenide (since the potential range below plateau No. 1 is not observed in chalcogen-free cells) and eventually accompanied by some amount of chloride. Therefore we assume that a general $Al_vNa_xNi_ySe_zCl_w$-type of compound is formed according to cathode reaction 5 and the overall cell reaction 6

$$v\,Al^{3+} + x\,Na^+ + w\,Cl^- + z\,Se^{2-} + y\,Ni + (3v + x - w - 2z)e^- \rightarrow Al_vNa_xNi_ySe_zCl_w \quad [5]$$

$$(3v + x - w - 6z)Al + 3x\,NaCl + (w - x)\,AlCl_3 + 3z\,Al_2Se_3 + 3y\,Ni \rightleftarrows 3Al_vNa_xNi_ySe_zCl_w \quad [6]$$

The small variation of the anode potential in Fig. 17 shows that the acidity of the melt remains essentially unchanged, *i.e.*, according to Eq., 6 $3x \approx w - x$ or $w \approx 4x$. Thus, to a good approximation Eq. 6 can be written

$$(v - x - 2z)Al + x\,NaCl + x\,AlCl_3 + z\,Al_2Se_3 + y\,Ni \rightleftarrows Al_vNa_xNi_ySe_zCl_{4x} \quad [7]$$

Due to the high affinity of the acidic NaCl-$AlCl_3$ melt for NaCl, x is presumably nearly zero, which means that essentially a $Al_vNi_ySe_z$ compound is formed.

The gradual decrease of the cathode potential in the range below plateau No. 1B indicates that $Al_vNi_ySe_z$ is formed by an insertion reaction. However, some of the decrease in potential is due to the slow reaction kinetics. This also explains the large hysteresis observed between first discharging and second charging (current reversal immediately re-establishes the value of the potential, see plateau No. 1C).

The high potential plateau, No. 2.—As in the sulfide case, either a Ni-Se-Cl compound or $NiCl_2$ is formed along plateau No. 2 during charging. The high potential data points agree within ~1 mV with calculated potentials for a $Ni/NiCl_2$-electrode, see Part I, Eq. 14. Figure 17 shows evidence, that also in the selenide system NaCl is "consumed" by the cathode reaction during first discharging.

The first charging curves of cathode and anode potentials display a discontinuity after ~525 coulombs had passed through the cell, see Fig. 16 and 17. It amounts to a partly discharging of the cell with ~180 coulombs, as estimated from Fig. 17. An aluminum dendrite might have drifted from the anode over to the cathode, causing it to be partly reduced. This is possible, since dendritic spongelike Al-deposits, with not too good attachment, are formed at the aluminum electrode during charging.[14] Rocking of the cell may cause some of the deposits to break off from the anode.

Summary and Conclusion

Al/NaCl-$AlCl_3$/Ni-felt secondary cells and corresponding cells with dissolved sulfide or selenide were investigated at 175°C.

Cathode reactions were studied by means of gravimetric analysis, Raman spectroscopy, and potentiometric measurements. The latter were compared with theoretical calculations performed by means of a model set up for Al/NaCl-$AlCl_3$-Al_2X_3/Ni-felt cells (X = S, Se).[1] Gravimetric analysis of electrolytes from fully charged cells (containing sulfide and cycled more than 100 times) has shown, that in the fully charged state, essentially all sulfide is present in the cathode.

The exchange of sulfide and selenide between cathode and the molten salt during charging and discharging have been studied by means of Raman spectroscopy. Sulfide was found to be "consumed" by the cathode reaction during charging and released to the melt during discharging. Due to higher signal-to-noise ratio clearer results could be obtained with the selenide system. During first charging all selenide present in the electrolyte was found to react with the nickel electrode in the form of Se^{2-}. During the subsequent discharging only about half of the selenide was released to the melt; the rest remaining in the electrode.

The potentiometric measurements were performed with slightly acidic NaCl-$AlCl_3$ melts containing ~0.51 m/o $AlCl_3$ and only small amounts of chalcogen.

Investigations on the chalcogenide-free cell showed that $NiCl_2$ forms during charging. During discharging, NaCl is "consumed" at the cathode.

In the sulfide system, the plateau of lowest potential, No. 1, is associated with formation/decomposition of essentially Ni_yS_z, possibly Ni_3S_2. The following plateau, No. 2, involves either $NiCl_2$ or a $Ni_yS_zCl_{2y-2z}$-compound with $y > (4.4 \pm 0.2) \cdot z$. The Ni_yS_z plateau displays a very good charge retention. The poor coulomb efficiency of ~80% for the first cycle is associated with plateau No. 2.

In acidic melts the sulfide species $Al_nS_{n-1}Cl_{2n+2-m}^{(n-m)-}$ were found to be almost saturated with sulfide-chloride double bridges of the type 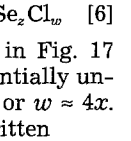 , corresponding to large values of m. At or nearby the cathode, $Al_2SCl_5^-$ species (the smallest ion of the assumed series), were needed to explain the experiments. However, in the bulk electrolyte sulfide species may exist with values of $n > 2$.

In the selenide system three sequential cathode reactions were observed. Compared with the sulfide system, cells containing selenide delivered a significant amount of charge at potentials below plateau No. 1. This charge/discharge range probably involves formation/decomposition of a $Al_vNi_ySe_z$ compound. In analogy with the sulfide results, plateau No. 1 (at ~0.85 V) is due to a Ni_ySe_z reaction, whereas plateau No. 2 (at ~1.275 V) is associated with either a Ni-Se-Cl compound or $NiCl_2$.

Acknowledgments

We wish to thank Lars Rosenmeier, F. W. Poulsen, Keld West, and Bo Vestergaard for help and valuable discussions, and the Danish Ministry of Energy, Director Ib Henriksens Fond, Thomas B. Thriges Fond, the Danish Technical Science Research Council, and the Technical University of Denmark for financial support.

Manuscript submitted Aug. 8, 1992; revised manuscript received Aug. 20, 1993.

REFERENCES

1. B. C. Knutz, H. A. Hjuler, R. W. Berg, and N. J. Bjerrum, *This Journal*, **140**, 3374 (1993).
2. H. A. Hjuler, R. W. Berg, and N. J. Bjerrum, *Power Sources*, **10**, 1 (1985); (Proceedings from the 14th International Power Sources Symposium 1984, Brighton, England).
3. B. Bugnet and D. Donoat, *Power Sources*, **10**, 377 (1985); (Proceedings from the 14th International Power Sources Symposium 1984, Brighton, England).
4. B. Bugnet and D. Donoat, Fr. Pat. 2,558,485 (1984).
5. R. W. Berg, H. A. Hjuler, and N. J. Bjerrum, *Inorg. Chem.*, **23**, 557 (1984).
6. H. A. Hjuler, R. W. Berg, and N. J. Bjerrum, Unpublished.
7. R. J. Bones, D. A. Teagle, S. D. Brooker, and R. C. Galloway, UK Pat. Appl. GB 2 164 786 A (1986).
8. R. W. Berg, S. von Winbush, and N. J. Bjerrum, *Inorg. Chem.*, **19**, 2688 (1980).
9. K. M. Abraham and J. E. Elliot, *This Journal*, **131**, 2211 (1984).
10. J-Y. Cherng, Ph.D. Thesis, Chemical Engineering Department, Brigham Young University, Provo, UT (1987).
11. H. A. Hjuler, S. von Winbush, R. W. Berg, and N. J. Bjerrum, *This Journal*, **136**, 901 (1989).
12. O. Wærnes and T. Østvold, *Acta. Chem. Scand.*, **A37**, 293 (1983).
13. B. V. Ratnakumar, S. Di Stefano, and G. Halpert, *This Journal*, **137**, 2991 (1990).
14. L. Qingfeng, H. A. Hjuler, R. W. Berg, and N. J. Bjerrum, *ibid.*, **137**, 593 (1990).

Oxidation of Acetonitrile-Based Electrolyte Solutions at High Potentials

An *In Situ* Fourier Transform Infrared Spectroscopy Study

Petr Krtil,[a] Ladislav Kavan,[a] and Petr Novák[b]

[a] *J. Heyrovský Institute of Physical Chemistry and Electrochemistry, Dolejškova 3, 182 23 Prague 8, Czech Republic*
[b] *Paul Scherrer Institute, CH-5232 Villigen PSI, Switzerland*

ABSTRACT

The oxidation of $LiAsF_6$/acetonitrile and $LiClO_4$/acetonitrile solutions containing 0.003-0.05*M* H_2O was studied on platinum and glassy carbon electrodes by *in situ* Fourier transform infrared spectroscopy. Both the solvent and the solute are unstable at potentials positive to *ca.* 2.2 V *vs.* SCE. The main oxidation product is CO_2. Other products detected are: acetamide ($LiAsF_6$/acetonitrile), ClO_2, and an unspecified "nitrogen oxide" ($LiClO_4$/acetonitrile). Carbon dioxide is formed via a reaction of acetonitrile with trace water as substantiated by the occurrence of an isotopic shift of the CO_2 stretching vibration when using $H_2{}^{18}O$. The rate of the CO_2 formation is increased by the presence of perchlorate anions and the Pt surface.

Research on lithium batteries[1] and photoelectrochemical cells[2,3] has demonstrated that the selection of a suitable electrolyte solution is as important as the design of electrodes. An appropriate aprotic solvent should be thermodynamically or at least kinetically stable over a wide potential range. Many experimental efforts are concentrated on the anodic stability of the electrolyte solutions since it controls various important practical parameters such as the overcharge stability of batteries, and photodegradation processes in solar cells employing n-type semiconductor electrodes.

Acetonitrile (AN) belongs to the most common class of aprotic solvents for electrochemical use.[4-14] The practically usable potential range of a Pt electrode extends up to about 2.3 to 2.7 V *vs.* SCE in perchlorate/AN solutions, but considerably higher potentials can be achieved using BF_4^- or PF_6^- salts as a supporting electrolyte.[4-6] Extremely high anodic potentials can be achieved on a Pt microelectrode in pure acetonitrile (with no added supporting electrolyte).[15] The limiting potential is hard to define precisely, *e.g.*, by an arbitrary level of faradaic current at a given potential program, since it may strongly depend on the purity of electrolyte solution, electrode pretreatments, etc.

The potential limiting reactions, both anodic and cathodic, are apparently initiated by the solute decomposition, but the mechanism of these reactions is a subject of considerable controversy.[4-15] The lower anodic stability of perchlorate/AN solutions has been attributed to the reactions[7]

$$ClO_4^- \rightarrow ClO_4^{\cdot} + e^- \quad [1]$$

$$ClO_4^{\cdot} + CH_3CN \rightarrow HClO_4 + CH_2CN^{\cdot} \quad [2]$$

$$2CH_2CN^{\cdot} \rightarrow NC{-}CH_2CH_2{-}CN \quad [3]$$

The primary product, the perchlorate radical $ClO_4^{\cdot}$ (Eq. 1), was reportedly identified by electron paramagnetic resonance (EPR).[10,11] This was, however, later questioned,[13] since the EPR spectrum can also be interpreted as that of chlorine dioxide formed either from $ClO_4^{\cdot}$ by the reaction

$$ClO_4^{\cdot} \rightarrow ClO_2 + O_2 \quad [4]$$

or by the decomposition of $HClO_4$ (cf. Eq. 2).[13] Besides ClO_2 and O_2, the formation of Cl^-,[9] O_3, and H_2O_2 was also mentioned.[7] The faradaic yield of perchloric acid (Eq. 2) is close to 100% as determined by acido-base titrations.[7-9,12] (By changing the solute, other anhydrous acids, *e.g.* HCl, can thus be prepared.[12] On the other hand, the succinonitrile (Eq. 3) was not detected,[4,11] and it was speculated that it is converted to pyrrole[7] (polypyrrole ?) or that reaction 2 leads to other oxidized species.[9] The formation of polyacetonitrile, $(-C(CH_3)=N-)_n$,[14] is another reaction pathway following from Eq. 2

$$CH_3CN + HClO_4 \rightarrow CH_3C^+{=}NH,ClO_4^- \quad [5]$$

$$n\,CH_3CN + CH_3C^+{=}NH,ClO_4^- \rightarrow HN{=}\underset{\displaystyle CH_3}{\underset{|}{C}}{-}(N{=}\underset{\displaystyle CH_3}{\underset{|}{C}}{-})_n\ N{=}\underset{\displaystyle CH_3}{\underset{|}{C^+}},ClO_4^- \quad [6]$$

Polyacetonitrile (ClO_4^- or BF_4^- doped) films gradually grow at the Pt anode at potentials more positive than 2.6 V *vs.* Ag/Ag^+ (0.01*M*). The —C=N— bond in polyacetonitrile is sensitive to hydrolytic splitting, leading to various fragments including acetamide.[14]